Available online at www.sciencedirect.com

ScienceDirect

journal homepage: http://www.elsevier.com/locate/rpor

Technical note

Comparison of surface dose delivered by 7 MV-unflattened and 6 MV-flattened photon beams

*Ashokkumar Sigamani**, *Arunai Nambiraj*

Department of Physics, School of Advanced Sciences, VIT University, Vellore 632014, India

ARTICLE INFO

Article history:
Received 17 March 2016
Received in revised form
7 October 2016
Accepted 20 December 2016

Keywords:
6 MV-flattened beam
7 MV-flattening filter-free beam
Surface dose
Parallel plate chamber
GafChromic film

ABSTRACT

Aim: The purpose of this study is to determine the central-axis dose in the buildup region and the surface dose delivered by a 6 MV flattened photon beam (6 MV-FB) and a higher energy unflattened (7 MV-FFF) therapeutic photon beam for different-sized square fields with open fields and modifying filters.

Materials and methods: The beams are produced by a Siemens Artiste linear accelerator with a NACP-02 ionization chamber and the dose is measured by using GafChromic film and two different, commonly used, dosimeters: a p-type photon semiconductor dosimeter (PFD) and a cylindrical ionization chamber (CC13).

Results: The results indicate that the surface dose increases linearly with FS for both open and wedged fields for the 6 MV-FB and 7 MV-FFF beams. The surface dose delivered by the 7 MV-UFB beam is consistent with that delivered by the 6 MV-FB beam for field sizes up to 10 cm × 10 cm, after which the surface dose decreases. The buildup dose for the 7 MV-UFB beam is slightly less than that for the 6 MV-FB beam for field sizes ranging from 5 cm × 5 cm to 15 cm × 15 cm. For both the 6 MV-FB and 7 MV-FFF beams, the measured surface dose clearly increases with increasing field size, regardless of the detector used in the measurement. The surface dose measured with the PFD dosimeter and the NACP-02 and CC13 chambers differ significantly from the results obtained when using GafChromic film. The 7 MV-FFF beam results in a slightly smaller surface dose in the buildup region compared with the 6 MV-FB beam.

Conclusions: The surface dose delivered by the higher energy 7 MV-FFF beam is less than that delivered by the energy-unmatched FFF beam in previously published works.

* *Corresponding author at*: Department of Physics, School of Advanced Sciences, VIT University, Vellore 632014, Tamil Nadu, India.
E-mail address: ashgknm@yahoo.co.in (A. Sigamani).

http://dx.doi.org/10.1016/j.rpor.2016.12.003

1. Introduction

The skin consists of three layers: the epidermis, the dermis, and subcutaneous fatty tissue. The thickness of the epidermis and dermis is 0.05–0.15 mm and 1–2 mm, respectively, in most locations. Under the dermis lies the subcutaneous fatty tissue. During radiotherapy, the skin-sparing effect of high-energy gamma and X-ray photons may be reduced or even lost if the beam is contaminated with electrons and/or low-energy photons. The dose accumulated at the air–skin boundary is known as the surface dose. For treating deep-seated tumors, the skin dose may be the factor that limits the delivery of high tumor doses[1] because of the possible biological complications of high skin doses in radiotherapy, such as desquamation, erythema, fibrosis, necrosis, and epilation. Epidemiologic studies have also found an association between radiation therapy and the onset of basal-cell carcinoma (BCC).[2–7]

The dose at the skin surface is the sum of two dose components[8]: the first component results from contaminant electrons from the air, in the collimator, and in the scattering material in the beam path,[9–12] and the second component comes from secondary electrons produced in the irradiated patient.[13] The dose from secondary electrons generated in the patient depends primarily on the size of the irradiated field but reaches an asymptotic value for large fields with sufficiently deep backscattering material to produce a lateral electron equilibrium.[8] However, the dose from contaminant electrons from the head depends strongly on the parameters of the clinical setup, such as field size, beam modifier (wedge), tray, block, and source-to-surface distance (SSD).[14–18]

In previous studies, the surface dose delivered by therapeutic photon beams was investigated by using one of various types of dosimeters, such as a thermoluminescence dosimeter,[19–21] radiochromic film,[22–25] and many types of parallel-plate ionization chambers.[26–30] Fixed-electrode-separation (parallel-plate) chambers are now commonly available and are also convenient for measuring the surface dose in clinical situations. However, their accuracy in the buildup region remains in doubt because a cavity perturbation from the chamber volume causes excess ionization. To obtain an accurate surface-dose measurement, the ionization reading must be corrected by considering the perturbation conditions. Velkley et al.[31] proposed using the correction factors derived from aluminum-walled extrapolation-chamber measurements obtained by adjusting the depth dose curves in the buildup region obtained from several types of fixed parallel-plate ionization chambers.

Recently, interest has increased in the use of flattening filter-free (FFF) X-ray photons. When the flattening filter is removed from the X-ray-beam path, photon production should be far more efficient and dose rate should increase substantially at the treatment target, which is especially beneficial for high-dose-per-fraction delivery techniques, such as stereotactic radiosurgery (SRS) and stereotactic body radiation therapy (SBRT).[32] Use of the FFF mode for SBRT lung-cancer treatment can significantly reduce beam-on time[33] and facilitate breath-hold or respiratory gating for more precise management of organ motion.[34] In addition, FFF X-rays are thought to offer dosimetric advantages, such as reduced peripheral doses, head scatter, and out-of-field scattered dose.[32,35–39] The energy-unmatched FFF beams contain more low-energy components and have softer energy spectra than the corresponding flattened beams, which can lead to increased dose in the buildup region.[40] Meanwhile, the energy-unmatched FFF photons undergo less head scatter because the flattening filter is absent from the gantry head of the linear accelerator, which may decrease the dose in the buildup region.[40] In the buildup region, where longitudinal electronic disequilibrium exists, these two competing factors determine the buildup dosimetric characteristics of the FFF photons. The first factor can reduce d_{max}, given that the mean energy of primary photons is reduced in the energy-unmatched FFF beams. However, the second factor will increase d_{max} because of the reduced contamination by head scattering of the FFF photons. The dose in the buildup region due to the FFF photons thus becomes interesting and may differ from that due to conventional flattened photons. Numerous publications discuss the dosimetry of energy-unmatched FFF beams produced by VARIAN accelerators.[32–39] However, relatively few dosimetric studies consider energy-increased FFF (7 MV-FFF) beams produced by the SIEMENS accelerator.[41]

The purpose of this study is to evaluate the central-axis dose in the buildup region and the surface dose delivered by a 6 MV flattened photon beam (6 MV-FB) and an energy-increased unflattened (7 MV-FFF) therapeutic photon beam for various square-field sizes with open fields. The beams are produced by a Siemens Artiste linear accelerator with a NACP-02 ionization chamber and are filtered by modifying filters. The dose measurements are made by using GafChromic film and also empirically by using two common dosimeters: a p-type photon semiconductor dosimeter (PFD) and a cylindrical ionization chamber (CC13).

2. Methods and materials

This study uses an Artiste (Siemens Medical Systems, USA) linear accelerator equipped with a 160 multi-leaf collimator. This system delivers 6 MV-FB and 7 MV-FFF beams with a PDD at 10 cm of 66.7% and 68.5%, respectively. Based on our commissioning data with a standard source-to-surface distance (SSD) of 100 cm and field size (FS) of 10 cm × 10 cm, d_{max} is 1.5 cm for 6 MV-FB and 2.1 cm for 7 MV-FFF.

The relative surface doses delivered by the 6 MV-FB and 7 MV-FFF beams were measured by using a plane-parallel ionization chamber (NACP-02, IBA-Scanditronix, Germany) with a DOSE 1 electrometer (IBA, Germany) in a solid-water-equivalent phantom with an adequate backscattering material. The solid-water phantom has a physical density of 1.04 g/cm^3. The NACP-02 chamber has a Mylar foil and graphite window with a combined thickness of 0.6 mm (104 mg/cm^2). The electrode spacing is 2.0 mm and the collecting-electrode diameter is 10 mm. The relative-surface-dose measurements were done with the 6 MV-FB and 7 MV-FFF beams aligned along the central axis, with square open fields of 5 cm × 5 cm, 8 cm × 8 cm, 10 cm × 10 cm, 15 cm × 15 cm, and 20 cm × 20 cm at 100 cm SSD, and with buildup depths extending from

the surface to just beyond the maximum depth. The surface dose was also measured for 30° and 60° wedged beams.

When measuring the surface dose, no charged-particle equilibrium exists because the ion chamber is located in the buildup region. This perturbs the plane-parallel ionization chambers, mainly because of undesired electron fluence that enters through the side wall of the chamber. This perturbation is corrected by using the method proposed by Gerbi and Khan, which gives a constant restricted mass stopping power ratio between the point of measurement and the dose maximum. To account for polarity effects, the measurements were done at both positive and negative voltage (+300 V and −300 V) for 6 MV-FB and 7 MV-FFF, which gave a polarity-correction factor of 0.99.

EBT2 (GafChromic) films were irradiated in a 30 cm × 30 cm × 30 cm solid-water phantom. The doses in the surface and buildup regions were measured with the film sandwiched tightly between slabs and irradiated while oriented parallel to the beam axis. The film pieces themselves were 6 cm × 25 cm. Each irradiation step delivered 200 monitor units. All films were scanned 24 h after irradiation. An Epson 10000XL (Epson America, Inc., Long Beach, USA) flatbed document scanner was used to scan the films following the manufacturer scanning protocol and recommendations. Epson software was used to scan the films in a transmission mode with a resolution of 75 dpi and with all image enhancements turned off. The images were saved as 48 bit TIFF files for further analysis. The surface dose of the scanned images was calculated by using OmniPro–I'mRT software (version 1.6; IBA dosimetry, Germany).

Surface dose was also measured empirically by using two common dosimeters: a PFD dosimeter and a CC13. The readings from each detector were assigned to the effective point of measurement for each individual detector. For the CC13 chamber, the effective point was determined automatically by the computerized scanning system. The effective points of measurement when measuring with the PFD dosimeter and with the NACP-02 chamber were assumed to be at the front surface and at the bottom of the entrance-window electrode, respectively.

3. Results

All the results given below for point-dose measurements are mean values from at least five measurements. The standard deviations are less than 1.5% and also partly crosschecked on different days to confirm that the initial results remain at least within ±1.5%.

3.1. *Surface dose vs. field size*

The surface dose within the buildup region increases linearly with field size by about 1% per cm^2 for both the 6 MV-FB and 7 MV-FFF photon beams. The fractional surface dose is defined as the surface dose for any field size divided by D_{max} for a 10 cm × 10 cm field. The relative surface dose is defined as the fractional surface dose divided by D_{max} for the corresponding field for which the dose was measured. The relative surface doses for 6 MV-FB and 7 MV-FFF beams for various field sizes were measured by using the NACP-02 chamber and EBT2 film, and the results are shown in Fig. 1. For the 6 MV-FB (7 MV-FFF) beam, the relative surface dose ranges from 30.39% to 48.02% (30.22–43.43%) when measured by NACP-02 and from 15.6% to 29.2% (14.4–24.6%) when measured by EBT2 film for field sizes from 5 cm × 5 cm to 30 cm × 30 cm (SSD is 100 cm for phantom surface). The relative surface doses for the 7 MV-FFF beam are consistent with those for the 6 MV-FB beam for field sizes up to 10 cm × 10 cm. However, as the field size increases above 10 cm × 10 cm, the relative surface dose with the 7 MV-FFF beam decreases compared with that with the 6 MV-FB beam.

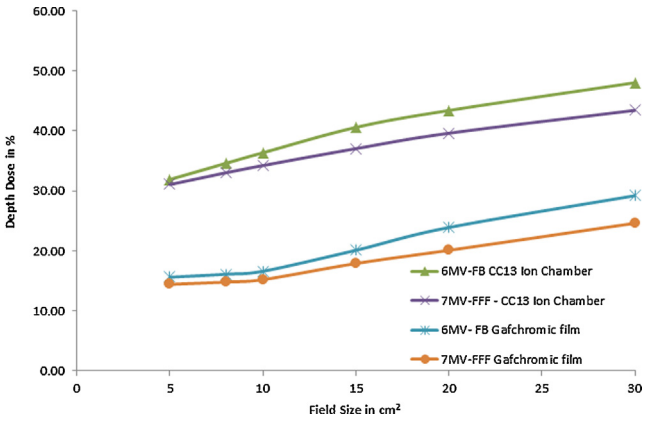

Fig. 1 – Relative surface dose of flattened and unflattened photon energy as a function of field size at a SSD of 100.0 cm.

3.2. *Doses at different buildup depths*

The buildup dose with 7 MV-FFF photons is slightly less than that with 6 MV-FB photons for the buildup depth with 5 cm × 5 cm to 15 cm × 15 cm fields (Fig. 2a–c and Table 1). For 7 MV-FFF and 6 MV-FB beams with a 10 cm × 10 cm field, the relative surface dose increases from 32.1% to 81.3% and from 34.20% to 85.6%, respectively, in the first 5 mm of buildup depth and from 32.1% to 93.8% and 34.20% to 97.37%, respectively, in the first 10 mm of buildup depth. The difference in buildup dose between the 6 MV-FB and 7 MV-FFF beams range from 0.3% to 6.3%, 0.2% to 6.7%, and 0.2% to 7.2% for 5 cm × 5 cm, 10 cm × 10 cm, and 15 cm × 15 cm fields, respectively (see Fig. 2d).

In the clinical work, we used a beam-modifying device (high-Z material) to alter the beam shape as required by the planning. Fig. 3 compares the surface dose for open and wedge fields with the 6 MV-FB and 7 MV-FFF beams. The surface dose for open fields with the 6 MV-FB and 7 MV-FFF beams are 34.6%, 36.4%, 40.6%, 43.4%, and 33%, 34.2%, 37%, 39.6%, respectively, for a 5 cm × 5 cm, 10 cm × 10 cm, 15 cm × 15 cm, and 20 cm × 20 cm field, respectively, at 100 cm SSD. The relative surface doses measured with 60° wedge filters are 24.7%, 30.2%, 35.6%, 40.2% and 21.5%, 26.9%, 30.4%, 33.7% for 6 MV-FB and 7 MV-FFF beams, respectively, and for a 5 cm × 5 cm,

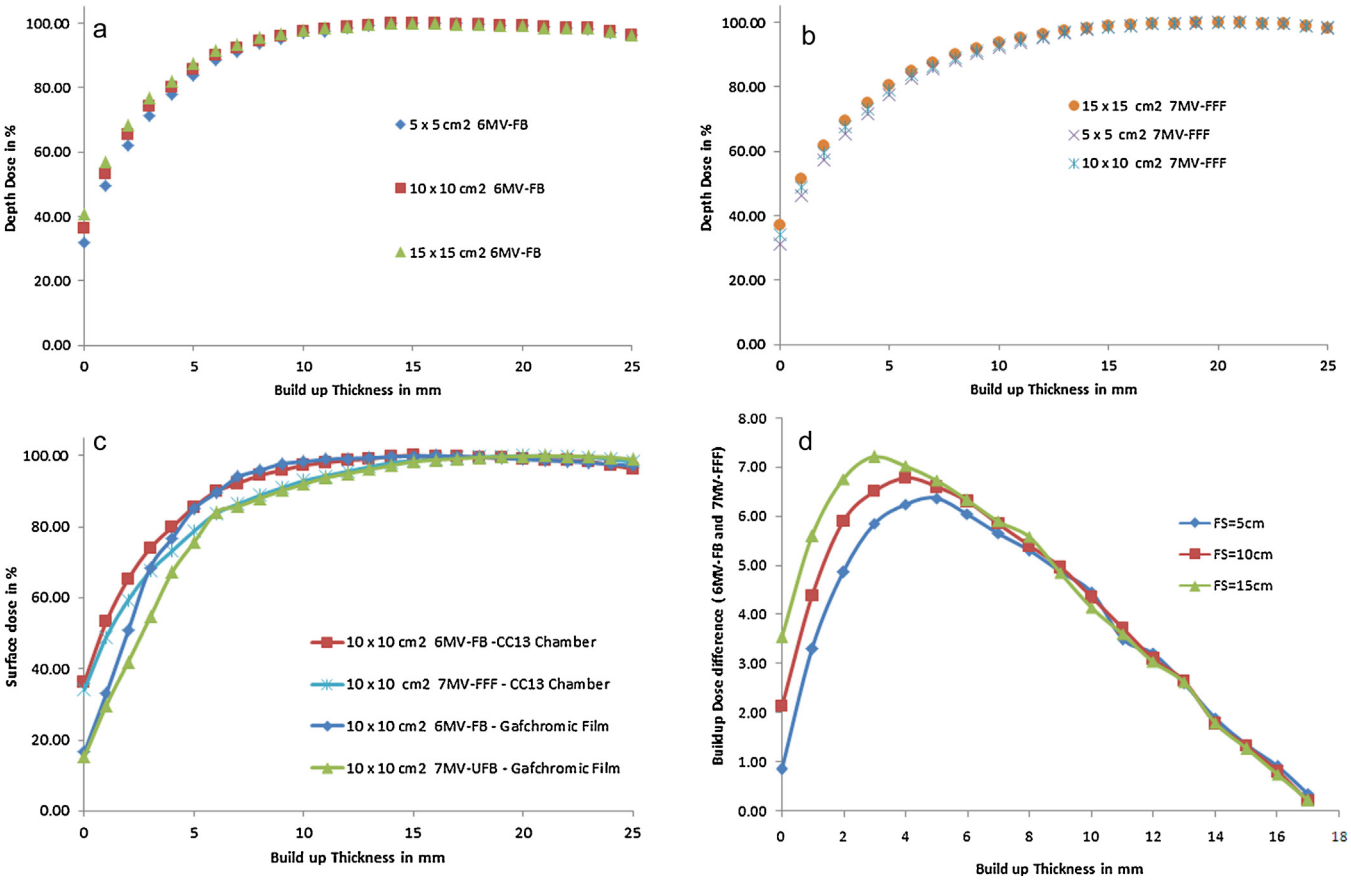

Fig. 2 – (a) Buildup dose delivered by 6 MV-FB beam for various buildup depths and field sizes. (b) Buildup dose delivered by 7 MV-FFF beam for various buildup depths and field sizes. (c) Buildup dose delivered by 7 MV-FFF beam delivered by 6 MV-FB beam for different buildup depths and for a 10 cm × 10 cm field. (d) Difference in buildup dose between 7 MV-FFF and 6 MV-FB beams and for various field sizes dependence on Beam-Modifying devices.

10 cm × 10 cm, 15 cm × 15 cm, and 20 cm × 20 cm field, respectively, at 100 cm SSD.

3.3. *Percent depth dose measured with various detectors*

Fig. 4a and b compares the depth-dose curves for the 6 MV-FB and 7 MV-FFF beams measured with various detectors for a 10 cm × 10 cm field. The three detectors measured the percent depth dose for the depth beyond the buildup region, and the results from the different detectors are consistent with each other. However, near the surface, the results of the three detectors differ significantly from the measured depth dose obtained with the EBT2 film (Table 2).

The surface dose measured with CC13 is 12.4% and 12.2% greater than when measured with NACP-02 for the 6 MV-FB and 7 MV-FFF beams, respectively, and for a 10 cm × 10 cm field at 100 cm SSD. The surface dose measured by PFD is 5.7% and 5.1% greater than when measured by NACP-02 for the 6 MV-FB and 7 MV-FFF beams, respectively, for 10 cm × 10 cm field size at 100 cm SSD. The surface dose measured by EBT2 film is 20.2% and 19.0% less than when measured by NACP-02 for the 6 MV-FB and 7 MV-FFF beams, respectively, and for a 10 cm × 10 cm field at 100 cm SSD.

Table 1 – Buildup dose delivered by 7 MV-FFF beam and 6 MV-FB beam for various buildup depths and field sizes.

Depth in mm	Field size in cm^2					
	5 × 5		10 × 10		15 × 15	
	6 MV-FB	7 MV-FFF	6 MV-FB	7 MV-FFF	6 MV-FB	7 MV-FFF
0	31.9	31.0	34.2	32.1	40.5	37.2
5	83.2	77.5	85.6	81.3	87.4	84.6
10	96.8	92.4	97.4	93.8	98.2	95.7

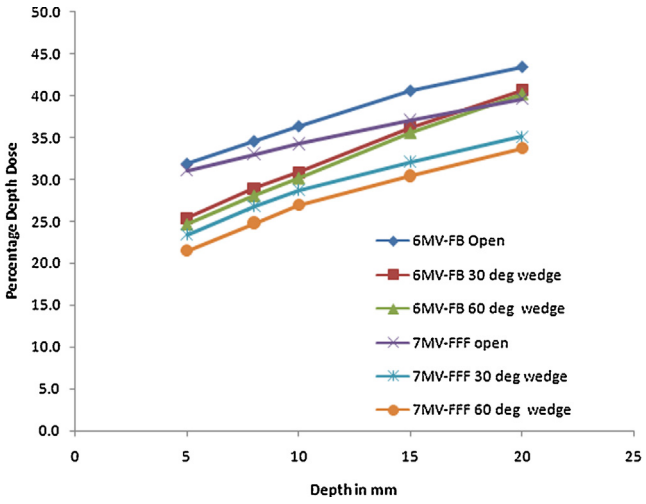

Fig. 3 – Relative surface dose delivered by flattened and unflattened beams as a function of various wedge filters at a SSD of 100.0 cm.

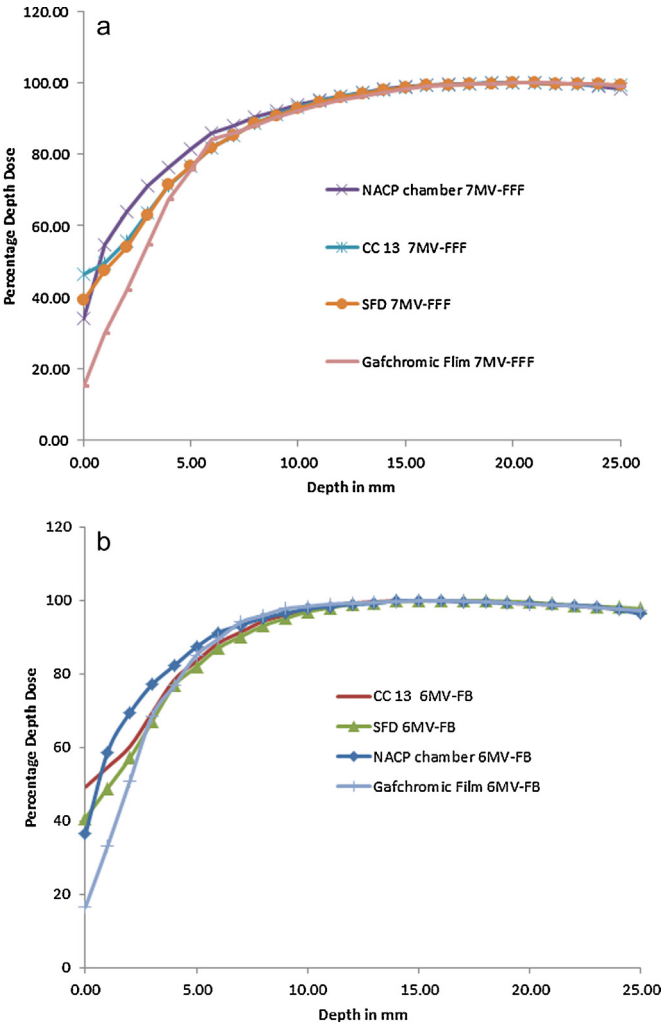

Fig. 4 – (a) Percent-depth dose curves obtained by using the GafChromic film, CC13, PFD, and NACP-02 chamber for 7 MV-FFF beams with 10 cm × 10 cm field size. (b) Percent-depth dose curves obtained by using the GafChromic film, CC13, PFD, and NACP-02 chamber for the 6 MV-FB beams with 10 cm × 10 cm field size.

4. Discussion

Although previous studies comprehensively described FFF beam dosimetric characteristics,[31–42] the dose in the buildup region is nevertheless well worth quantifying, and its clinical impact is worth pursuing. For the high-energy photons used in conventional radiotherapy, skin dose may be less of a concern because of the skin-sparing effect, which allows high-energy photons to be delivered to deep-seated tumors without exceeding the skin tolerance for radiation. However, for unconventional hypofractionated (SBRT or SRS) delivery, where the fractional dose is extremely high, an acute skin reaction can occur.[34] Therefore, it is clinically important to analyze and compare the characteristics of the buildup dose for both the 6 MV-FB and 7 MV-FFF beams.

The measurements on the surface area with a parallel-plane ionization chamber, however, overestimate the surface dose because the chamber is perturbed, as described in Methods and Materials. Upon applying the correction factor, the

Table 2 – Comparison of relative surface doses measured with different types of dosimeter for 6 MV-FB and 7 MV-FFF.

Type of detectors	Field size in cm^2				
	5 × 5	10 × 10	15 × 15	20 × 20	30 × 30
NACP-02					
6 MV-FB	34.6	36.4	40.6	44.2	56.4
7 MV-FFF	33	34.2	37	40.1	46.5
GafChromic film					
6 MV-FB	15.6	16.6	20.1	25.3	36.5
7 MV-FFF	14.4	15.2	17.9	24.5	29.9
CC13					
6 MV-FB	44.9	49.2	53.2	57.8	64.4
7 MV-FFF	43.6	46.6	49.9	51.9	60.1
SFD					
6 MV-FB	36.5	40.8	45.8	49.3	58.6
7 MV-FFF	36.1	39.5	43.4	48.6	60.3

open-field doses measured for 6 MV-FB and 7 MV-FFF beams and 10 cm × 10 cm fields decrease from 43.30% and 41.17% to 34.20% and 32.10%, respectively. The corrected values for 6 MV-FB are similar to the 33.3% surface doses measured by Parsai et al.[43] with an extrapolation chamber at a depth of 0.5 mm and with the same field size and energy.

The surface dose increases linearly with field size for both the 6 MV-FB and 7 MV-FFF beams, which is due to increased electron emission from the collimator and from air. The measured surface doses for the 6 MV-FB and 7 MV-FFF beams plotted in Fig. 1 against equivalent square show significant difference between the FB and FFF modes. These results reveal the important contribution of the flattening filter to the surface dose for field sizes exceeding 10 cm × 10 cm. Removal of the flattening filter leads to a decrease in head scatter[39,40,44] for field sizes exceeding 10 cm × 10 cm. These results indicate that the reduced surface dose for the 7 MV-FFF beam due to reduced head scatter for field sizes above 10 cm × 10 cm is due to the absence of the flattening filter in the field.

The beam-hardening effect imposed by the flattening filter helps reduce the surface or skin dose. However, the filter also produces a large amount of scattered radiation that tends to deposit energy at shallow depths, thereby adding to the surface dose, and this effect depends strongly on field size. Cashmore[45] and Kragl et al.[46] found that the buildup dose increases with depth in solid water and the surface dose and buildup-region dose delivered by the FFF beam produced by an Elekta Precise Linac slightly exceeds that delivered by the flattened beam from the same source. These results are not consistent with the results presented herein, which were obtained with the Siemens Artiste Linac. The surface dose and buildup-region dose delivered by the unflattened beam may be lower because of the increased photon energy. Our results confirm that the surface dose and buildup-region dose delivered by an equivalent-quality unflattened beam are less than those delivered by an unmatched equivalent-quality unflattened beam.

Similar to the skin dose for an open field, the skin dose for a wedge field increases with increasing field size. Fig. 4 shows the variation of surface dose with physical wedge filters positioned in the beam path. The results are compared with those of the open and wedge fields with the 6 MV-FB and 7 MV-FFF photon beams. At both energies, the surface doses for the wedge and open fields differ. At both energies, the physical wedge tends to decrease the surface dose relative to the dose for the open field. A physical wedge can both eliminate the upstream electrons and generate electrons itself. The number of electrons produced in the wedge appears to be less than the number of electrons eliminated by the wedge; thus, these results are consistent with those of previous studies.[47,48]

For both the 6 MV-FB and 7 MV-FFF photon beams, the surface dose clearly increases with increasing field size, regardless of the detector used to make the measurement. This result is mainly due to the increasing number of scattered electrons in the air and collimator. The surface dose measured by the PFD dosimeter and the CC13 chamber differ greatly from that measured by the NACP-02 chamber. For a 10 cm × 10 cm field size, the PFD and CC13 dosimeters measured high percentage surface doses of about 40.7% and 49.2% for the 6 MV-FB beam and 39.2% and 46.7% for the 7 MV-FFF beam, respectively. These two detectors may have detected a significant number of low-energy electrons from the non-electronic equilibrium situation in the buildup region. Moreover, at some point in the measurement, and in particular close to the phantom surface, a portion of each detector was above the water level, which also contributes to the non-equilibrium situation. For a field size of 10 cm × 10 cm, Apipunyasopon et al.[48] scaled down the excessive response to the surface dose by using the correction factors 0.294 and 0.378 for the CC13 chamber and PFD, respectively. Upon applying the correction factors, the surface doses delivered by the 6 MV-FB beam and the 7 MV-FFF beam are 14.5% (CC13), 15.4% (PFD), and 13.7% (CC13), 14.8% (PFD), respectively for 10 cm × 10 cm field. These corrected surface doses are consistent with published values.

The high spatial resolution and low spectral sensitivity provided by radiochromic films make them ideal for measuring dose distributions in regions in which a radiation field produces a high dose gradient. As expected, surface dose increases with field size due to extra electron contamination and photon head scatter. Table 2 shows the surface doses for various field sizes as measured by EBT2 GafChromic film and by the NACP-02 chamber. The NACP-02 chamber overestimates the dose by 20% compared with the EBT2 GafChromic film for both the flattened and unflattened photon beams. We compare these results with those of Butson et al.,[49] who measured surface dose with GafChromic film type MD-55. The data obtained in the present work are consistent with the results obtained with the Attix chamber to within 3% for 6 MV high-energy photon beams. The surface dose measured by GafChromic film models HD-810, EBT, HS, and XR for a 6 MV photon beam was investigated more comprehensively by Devic et al.[50]

5. Conclusion

A 7 MV-unflattened beam delivers a slightly less surface dose in the buildup region than a 6 MV flattened beam. The surface dose delivered by the higher-energy 7 MV-FFF beam is less than that delivered by energy-unmatched FFF beams in previously published works. However, the difference is not substantial and may be clinically insignificant. Knowledge of the dosimetric characteristics in the buildup region and of the surface dose delivered by 7 MV-FFF beams is useful for implementations of IMRT, SRS, and SBRT.

Conflict of interest

None declared.

Financial disclosure

None declared.

REFERENCES

1. Lee N, Chuang C, Quivey JM, et al. Skin toxicity due to intensity-modulated radiotherapy for head-and-neck carcinoma. *Int J Radiat Oncol Biol Phys* 2002;**53**(3):630–7.
2. Shore RE. Overview of radiation-induced skin cancer in humans. *Int J Radiat Biol* 1990;**57**:809–27.
3. Karagas MR, McDonald JA, Greenberg ER, et al. Risk of basal cell and squamous cell skin cancers after ionizing radiation therapy. *J Natl Cancer Inst* 1996;**88**(24):1848–53.
4. Lichter MD, Karagas MR, Mott LA, Spencer SK, Stukel TA, Greenberg ER. Therapeutic ionizing radiation and the incidence of basal cell carcinoma and squamous cell carcinoma. *Arch Dermatol* 2000;**136**(8):1007–11.
5. Perkins JS, Liu Y, Mitby PA, et al. Nonmelanoma skin cancer in survivors of childhood and adolescent cancer: a report from the childhood cancer survivor study. *J Clin Oncol* 2005;**23**(16):3733–41.
6. Levi F, Moeckli R, Randimbison L, Te VC, Maspoli M, La Vecchia C. Skin cancer in survivors of childhood and adolescent cancer. *Eur J Cancer* 2006;**42**(5):656–9.
7. Schwartz JL, Kopecky KJ, Mathes RW, Leisenring WM, Friedman DL, Deeg HJ. Basal cell skin c cancer after total-body irradiation and hematopoietic cell transplantation. *Radiat Res* 2009;**171**(2):155–63.
8. Bjärngard BE, Vadash P, Zhu T. Doses near the surface in high-energy X-ray beams. *Med Phys* 1995;**22**:465–8.
9. Ling CC, Biggs PJ. Improving the buildup and depth-dose characteristics of high energy photon beams by using electron filters. *Med Phys* 1979;**6**:296–301.
10. Mackie TR, Scrimger JW. Contamination of a 15-MV photon beam by electrons and scattered photons. *Radiology* 1982;**144**:403–9.
11. Nilsson B, Brahme A. Electron contamination from photon beam collimators. *Radiother Oncol* 1986;**5**:235–44.
12. Beauvais H, Bridier A, Dutreix A. Characteristics of contamination electrons in high energy photon beams. *Radiother Oncol* 1993;**29**:308–16.
13. Nizin PS. Electronic equilibrium and primary dose in collimated photon beam. *Med Phys* 1993;**20**:1721–9.
14. McCullough EC. A measurement and analysis of buildup region dose for open field photon beams (cobalt-60 through 24 MV). *Med Dosim* 1994;**19**:5–14.
15. Fontenla DP, Napoli JJ, Hunt M, Fass D, McCormick B, Kutcher GJ. Effects of beam modifiers and immobilization devices on the dose in the build-up region. *Int J Radiat Oncol Biol Phys* 1994;**30**:211–9.
16. Klein EE, Purdy JA. Entrance and exit dose regions for a Clinac-2100C. *Int J Radiat Oncol Biol Phys* 1993;**27**:429–35.
17. McParland PJ. The effects of a universal wedge and beam obliquity upon the central axis dose buildup for 6-MV X-rays. *Med Phys* 1991;**18**:740–3.
18. Jani SK, Pennington EC. Depth dose characteristics of 24-MV X-ray beams at extended SSD. *Med Phys* 1991;**18**:292–4.
19. Nilsson B, Sorcini B. Surface dose measurements in clinical photon beams. *Acta Oncol* 1989;**28**:537–42.
20. Stathakis S, Li J-S, Paskalev K, et al. Ultra-thin TLDs for skin dose determination in high energy photon beams. *Phys Med Biol* 2006;**51**:3549–67.
21. Hsu S-H, Roberson P-L, Chen Y, et al. Assessment of skin dose for breast chest wall radiotherapy as a function of bolus material. *Phys Med Biol* 2008;**53**:2593–606.
22. Butson M-J, Cheung T, Yu P-K-N, et al. Variations in skin dose associated with linac bed material at 6 MV X-ray energy. *Phys Med Biol* 2002;**47**:N25–30.
23. Paelinck L, Wagter C-D, Esch A-V, et al. Comparison of build-up dose between Elekta and Varian linear accelerators for high-energy photon beams using radiochromic film and clinical implications for IMRT head and neck treatments. *Phys Med Biol* 2005;**50**:413–28.
24. Price S, Williams M, Butson M, et al. Comparison of skin dose between conventional radiotherapy and IMRT. *Australas Phys Eng Sci Med* 2006;**29**:272–7.
25. Devic S, Seuntjens J, Abdel-Rahman W, et al. Accurate skin dose measurements using radiochromic film in clinical applications. *Med Phys* 2006;**33**:1116–24.
26. Nilsson B-O, Montelius A. Fluence perturbation in photon beams under nonequilibrium conditions. *Med Phys* 1986;**13**:191–5.
27. David E, Mellenberg J-R. Determination of build-up region over-response corrections for a Markus-type chamber. *Med Phys* 1990;**17**:1041–4.
28. Gerbi B-J, Khan F-M. Measurement of dose in the buildup region using fixed-separation plane-parallel ionization chambers. *Med Phys* 1990;**17**:17–26.
29. Lamb A, Blake S. Investigation and modeling of the surface dose from linear accelerator produced 6 and 10 MV photon beams. *Phys Med Biol* 1998;**43**:1133–46.
30. Carl J, Vestergard A. Skin damage probabilities using fixation materials in high-energy photon beams. *Radiother Oncol* 2000;**55**:191–8.
31. Velkley D-E, Manson D-J, Purdy J-A, et al. Build-up region of megavoltage photon radiation sources. *Med Phys* 1975;**2**: 14–9.
32. Georg D, Knoos T, McClean B. Current status and future perspective of flattening filter free photon beams. *Med Phys* 2011;**38**:1280–93.
33. Wang Y, Golden N, Ting JY. Treatment planning study: flattening filter free X-rays vs. conventional flattened X-rays for stereotactic body radiation therapy of stage 1A non-small cell lung cancer (NSCLC). In: *Presented at the 2011 annual meeting of the Radiological Society of North America*. 2011.
34. Vassiliev ON, Kry SF, Chang JY, et al. Stereotactic radiotherapy for lung cancer using a flattening filter free linac. *J Appl Clin Med Phys* 2009;**10**:14–21.
35. Kragl G, Baier F, Lutz S, et al. Flattening filter free beams in SBRT and IMRT: dosimetric assessment of peripheral doses. *Z Med Phys* 2011;**21**:91–101.
36. Kry SF, Vassiliev ON, Mohan R. Out-of-field photon dose following removal of the flattening filter from a medical accelerator. *Phys Med Biol* 2010;**55**:2155–66.
37. Vassiliev ON, Titt U, Ponisch F, et al. Dosimetric properties of photon beams from a flattening filter free clinical accelerator. *Phys Med Biol* 2006;**51**:1907–17.
38. Wang Y, Gajdos S, Tendulkar R, et al. Application of non-flat beams for breast radiotherapy using direct aperture optimization. *Med Phys* 2010;**37**:3215.
39. Ashokkumar S, Nambi Raj NA, Sinha SN, et al. Comparison of head scatter factor 6 MV and 10 MV flattened (FB) and unflattened (FFF) photon beam using indigenously designed columnar mini phantom. *J Med Phys* 2014;**39**:184–91.
40. Ashokkumar S, Nambiraj A, Sinha SN, et al. Measurement and comparison of head scatter factor for 7 MV unflattened (FFF) and 6 MV flattened photon beam using indigenously designed columnar mini phantom 2015. *Rep Pract Oncol Radiother* 2015;**20**:170–80;
Khan FM. *Physics of radiation therapy*. 3rd ed. Philadelphia: Lippincott Williams & Wilkins; 2003.
41. Huang Y, Siochi RA, Bayouth JE. Dosimetric properties of a beam quality-matched 6 MV unflattened photon beam. *JACMP* 2012;**13**:71–81.
42. Ishmael Parsai E, Shvydka D, Pearson D, Gopalakeishnan M, Feldmeier JJ. Surface and build-up region dose analysis for clinical radiotherapy photon beams. *Appl Radiat Isot* 2008;**66**(10):1438–42.

43. Hall EJ, Wuu CS. Radiation-induced second cancers: the impact of 3D-CRT and IMRT. *Int J Radiat Oncol Biol Phys* 2003;**56**:83–8.
44. Cashmore J. The characterization of unflattened photon beams from a 6 MV linear accelerator. *Phys Med Biol* 2008;**53**:1933–46.
45. Kragl G, af wetterstdt S, Knausl B, et al. Dosimetric characteristics of 6 and 10 MV unflattened photon beams. *Radiother Oncol* 2009;**93**:141–6.
46. Kim S, Liu CR, Zhu TC, Palta JR. Photon beam skin dose analyses for different clinical setups. *Med Phys* 1998;**25**(6):860–6.
47. Rapley P. Surface dose measurement using TLD powder extrapolation. *Med Dosim* 2006;**31**(3):209–15.
48. Apipunyasopon L, Srisatit S, Phaisangittisakul N. An investigation of the depth dose in the build-up region, and surface dose for a 6-MV therapeutic photon beam: Monte Carlo simulation and measurements. *J Radiat Res (Tokyo)* 2013;**54**:374–82.
49. Butson MJ, Yu PKN, Metcalfe EM. Extrapolated surface dose measurements with radiochromic film. *Med Phys* 1999;**26**(3):485–7.
50. Devic S, Seuntjens J, Abdel-Rahman W, Evans M, Olivares M, Podgorsak EB. Accurate skin dose measurements using radiochromic film in clinical applications. *Med Phys* 2006;**33**(4):1116–23.